Jurnal Nasional Teknik Elektro dan Teknologi Informasi
Volume 15 Number 1 February 2026

DOI: 10.22146/jnteti.v15i1.22694

Fuzzy Control of Three-Phase Induction Motor Using Mitsubishi PLC: Experimental Study

Nanang Rohadi[1], Liu Kin Men[2], Akik Hidayat[3]

[1] Department of Electrical Engineering, Faculty of Mathematics and Natural Sciences, Universitas Padjadjaran, Sumedang, Jawa Barat 45363, Indonesia
[2] Department of Physical Sciences, Faculty of Mathematics and Natural Sciences, Universitas Padjadjaran, Sumedang, Jawa Barat 45363, Indonesia
[3] Department of Informatics and Computer Sciences, Faculty of Mathematics and Natural Sciences, Universitas Padjadjaran, Sumedang, Jawa Barat 45363, Indonesia

[Received: 7 July 2025, Revised: 7 October 2025, Accepted: 2 February 2026]
Corresponding Author: Nanang Rohadi (email: nanang.rohadi@unpad.ac.id).

ABSTRACT — Three-phase induction motors are extensively deployed in industrial automation due to their robustness, simplicity, and efficiency. Nevertheless, maintaining speed stability under dynamically varying loads remains a significant control challenge. This study investigated the design and implementation of a fuzzy logic-based speed control system fully embedded within a Mitsubishi FX3U-64M programmable logic controller (PLC), eliminating the dependency on external software platforms. The system integrated a rotary encoder for real-time speed feedback, an FX2N-2DA digital-to-analog converter for signal output, and a Mitsubishi FR-E520 inverter for frequency and voltage regulation. The fuzzy controller utilized two input variables, speed error and rate of change, which were fuzzified and processed through a Mamdani-type inference mechanism. All fuzzy operations, including rule evaluation and centroid-based defuzzification, were executed using ladder diagram programming via GX Works2. Experimental validation was performed across five speed references (300 to 1200 rpm) and varying mechanical loads (0.5–1.5 kg). The controller consistently achieved steady-state errors below 1% in no-load conditions and below 0.5% under load, with recovery times ranging from 1.5 to 6.75 s. These results demonstrate that the proposed PLC-based fuzzy controller provides a responsive, accurate, and fully integrable solution for real-time industrial motor speed regulation under variable operating conditions.

KEYWORDS — Fuzzy Logic Control, Mitsubishi PLC, Three-Phase Induction Motor, Industrial Automation, Speed Regulation, Real-Time Control.

I. INTRODUCTION

Three-phase induction motors are the most widely used electric motors in modern industrial applications due to their robustness, high efficiency, and low maintenance cost [1]–[3]. Despite these advantages, such motors exhibit limitations in maintaining constant speed under varying load conditions [4]. Load-induced torque fluctuations often result in speed instability, potentially compromising the overall stability of industrial processes [5]–[6].

In industrial practice, motor speed regulation is often performed manually or via conventional control methods such as proportional–integral–derivative (PID) controllers. However, conventional PID controllers are less effective in managing nonlinearities and time-varying dynamics inherent in many real-world systems [7]–[8]. This limitation highlights the need for more adaptive and intelligent control strategies capable of addressing such complexities.

Although fuzzy logic has been widely recognized as an effective strategy for handling nonlinearities and parameter uncertainties in control systems without requiring explicit mathematical models [9]–[10], the majority of implementations reported in the literature remain limited to simulation platforms such as MATLAB or LabVIEW [11]. While these simulation-based studies are useful for conceptual validation, they do not fully capture the complexity and constraints encountered in industrial environments, particularly under variable loading conditions.

Only a limited number of investigations have explored the direct implementation of fuzzy logic controllers on industrial-grade hardware such as programmable logic controllers (PLC). Moreover, most of these works have focused on nominal or no-load conditions, with insufficient consideration of dynamic load variations that are common in real-world applications. This lack of comprehensive experimental validation under realistic operating conditions highlights a critical gap between simulation-oriented studies and the requirements of practical industrial deployment.

To address this limitation, the present work proposes the design and implementation of a fuzzy logic-based speed control system for a three-phase induction motor, fully embedded within a Mitsubishi FX3U-64M PLC. In contrast to prior approaches, the proposed system eliminates the dependency on external computing platforms by implementing the entire fuzzy control algorithm using ladder diagram programming within GX Works2. This architecture not only reduces system complexity but also enhances integration with existing automation infrastructures.

In addition, the proposed controller is experimentally validated under both no-load and dynamic load conditions, with mechanical load variations ranging from 0.5 kg to 1.5 kg applied to the motor shaft. Such validation provides a more rigorous assessment of the system's adaptability, steady-state accuracy, and transient response, thereby demonstrating its suitability for industrial environments where load disturbances are inevitable.

The novelty of this study includes the complete implementation of a fuzzy logic controller within an industrial-grade PLC without reliance on external software and the comprehensive experimental validation of its performance under dynamic load conditions. These contributions advance the state of the art by bridging the gap between simulation-based studies and practical industrial applications, offering a compact, adaptive, and deployable control solution for real-time motor speed regulation.

II. SYSTEM DESIGN AND METHODOLOGY

A. SYSTEM CONFIGURATION

The system configuration proposed in this study was designed to implement real-time speed control of a three-phase induction motor using fuzzy logic embedded directly within the Mitsubishi FX3U-64M PLC. This system integrated both hardware and software components to facilitate seamless data acquisition, fuzzy logic processing, and control signal output in an industrial environment.

The core components of the system were organized into six main modules: the Mitsubishi FX3U-64M PLC serving as the central controller; the Mitsubishi FR-E520 inverter regulating power supply to the motor; the FX2N-2DA digital-to-analog converter (DAC) module for converting digital signals into analog control voltages; a 0.24 kW, 380V, 50Hz three-phase induction motor acting as the actuator; the Koyo TRD-J100SW rotary encoder providing real-time speed feedback; and the GOT1000 human machine interface (HMI) for real-time monitoring and set point configuration. These components were interconnected to form a closed-loop control system capable of responding adaptively to load variations. The overall system interconnection is illustrated in Figure 1, which presents the block diagram of the fuzzy logic speed control system as implemented in this study.

The motor's speed was sensed by the rotary encoder and transmitted as pulse signals to the high-speed counter input of the PLC. The PLC computed the actual motor speed and compared it with the set point input provided via the HMI. The resulting error and delta error values were used as inputs to the fuzzy logic controller. The fuzzy controller processed these inputs to generate a digital output value (DV), which was then converted into a 0–10 V analog signal by the FX2N-2DA DAC module. This analog signal was passed to the Mitsubishi FR-E520 inverter, which adjusted the voltage and frequency supplied to the motor, thereby regulating the motor speed precisely in real time.

The entire fuzzy logic processing, including error calculation, fuzzification, rule evaluation, defuzzification, and output scaling, was fully implemented within the PLC using ladder diagram programming via GX Works2 software. This configuration not only supports adaptive real-time control but also facilitates seamless integration with industrial automation systems without the need for external computing devices, thereby offering a practical and efficient control solution.

Figure 2 depicts the overall configuration of the fuzzy logic-based speed control system for a three-phase induction motor, presented in a block diagram format. The system integrated multiple hardware components, each with a specific role in achieving real-time, closed-loop motor speed regulation. The GOT1000 HMI was used to input the reference speed and monitor system performance. The control logic was fully executed within the Mitsubishi FX3U-64M PLC, performing critical operations, such as speed calculation, error and delta error computation, fuzzification, rule-based inference, and defuzzification using ladder diagram programming.

To generate analog control signals, the FX2N-2DA DAC module converted the PLC's digital output into a 0–10 V analog voltage. This signal was transmitted to the Mitsubishi FR-E520 inverter, which modulated the frequency and amplitude of the power supplied to the motor. The controlled device was a 0.24 kW, 380 V, 50 Hz three-phase induction motor, whose shaft speed was continuously measured using a

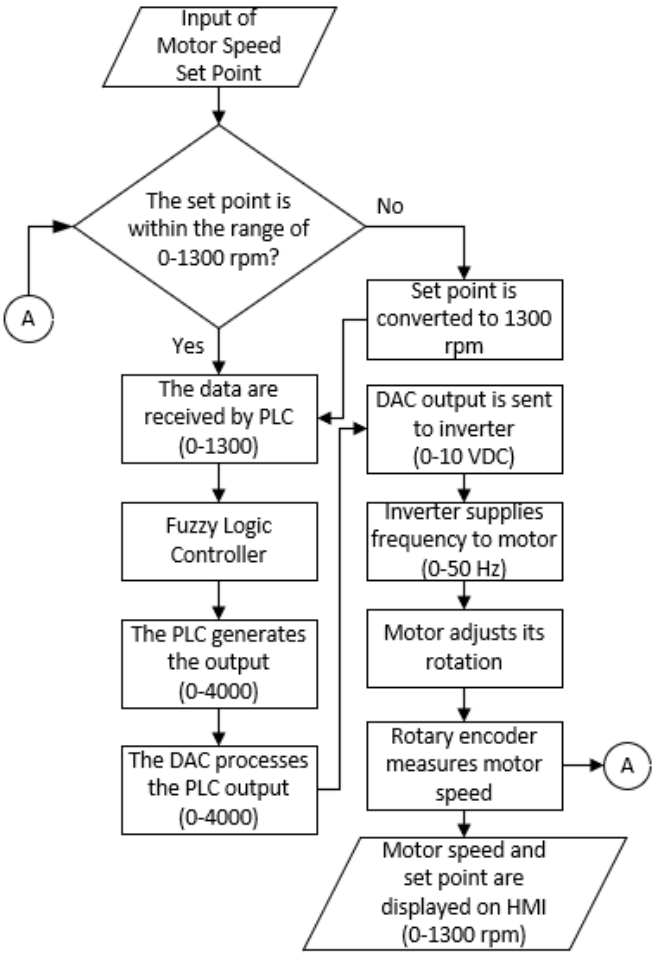

Figure 1. Block diagram of the PLC-based fuzzy logic speed control system for a three-phase induction motor.

Koyo TRD-J100SW rotary encoder. The encoder provided high-speed pulse feedback to the PLC's high-speed counter input, enabling accurate real-time speed measurement. This system configuration formed a fully embedded, adaptive control architecture that eliminated the need for external computing platforms, making it highly suitable for industrial automation applications where responsiveness, precision, and seamless integration with existing infrastructures are critically required.

B. FUZZY CONTROL STRUCTURE

The fuzzy logic-based speed control system for the three-phase induction motor was designed to address system uncertainty, nonlinear dynamics, and real-time load fluctuations. The entire fuzzy algorithm was independently implemented within the Mitsubishi FX3U-64M PLC using ladder diagram programming via GX Works2 software, without reliance on external platforms such as MATLAB or LabVIEW. This approach results in an efficient, responsive, and fully integrable control system tailored for industrial automation environments [12]–[13]. The fuzzy controller consists of three primary stages: fuzzification, rule evaluation (inference), and defuzzification [14]–[16]. These stages were executed in a coordinated sequence within the PLC to generate control signals for the inverter based on the real-time operating condition of the system.

1) INPUT VARIABLE DEFINITION

The effectiveness of fuzzy control heavily depends on the appropriate selection of input variables. Two key input

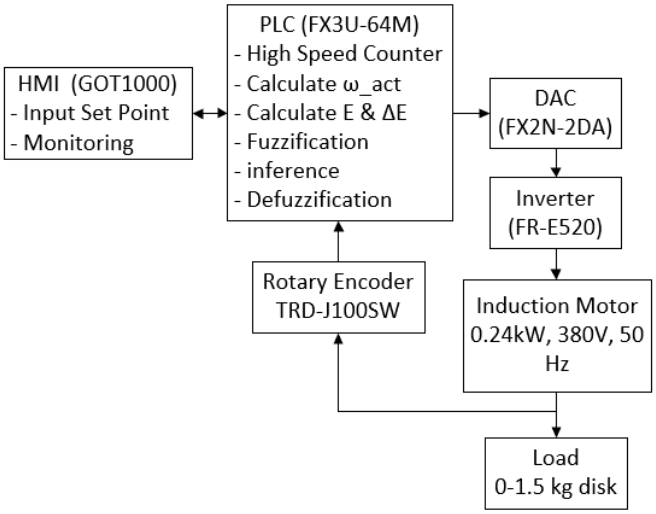

Figure 2. System architecture of the fuzzy logic-based motor speed controller.

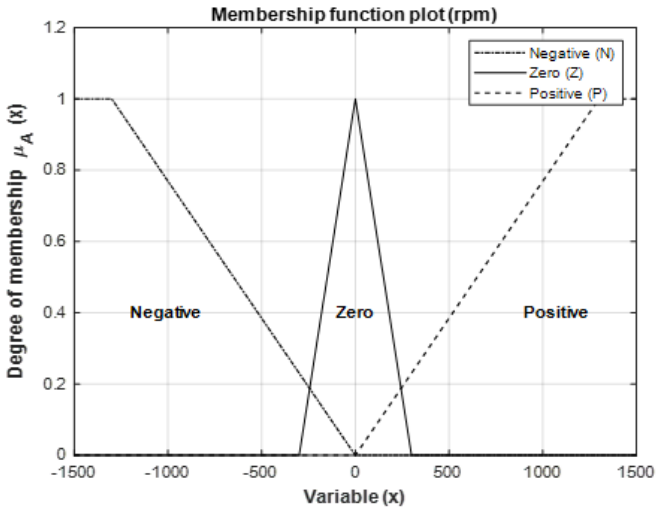

Figure 3. Triangular membership functions for input variables Error/ΔError.

variables were employed: the speed error $E(k)$ and the change in speed error $\Delta E(k)$. These variables capture the dynamic behavior of the system in real time and form the basis for fuzzy decision-making.

Speed error is defined as the difference between the reference speed $\omega_{set}(k)$, entered via the HMI, and the actual speed $\omega_{act}(k)$, measured by the rotary encoder [16]:

$$E(k) = \omega_{set}(k)[rpm] - \omega_{act}(k)[rpm]. \quad (1)$$

A positive error ($E > 0$) indicates the motor is running slower than desired, while a negative error ($E < 0$) signifies overspeed. A zero error implies the motor operates precisely at the set point.

The change in error, or delta error, represents the variation of the speed error across consecutive control cycles:

$$\Delta E_k = E_k - E_{k-1}. \quad (2)$$

A positive ΔE indicates diverging system behavior (error increasing), while a negative ΔE shows convergence toward the set point (error decreasing).

2) FUZZIFICATION

Fuzzification is the initial stage of fuzzy logic control, converting crisp input values into linguistic representations via fuzzy sets. This process enhances the controller's flexibility in dealing with nonlinearities and uncertainties. Both input variables, namely the instantaneous speed error $E(k)$ and the change in error $\Delta E(k)$, were translated into fuzzy linguistic terms through a process known as fuzzification. This was achieved by mapping each crisp input value to predefined fuzzy sets using triangular membership functions. In this study, three linguistic categories were defined for each input variable: negative (N), zero (Z), and positive (P). For the error input, the domain spanned from −1300 to 1300 rpm, with the fuzzy subsets defined as negative (−1300 to 0 rpm), zero (−300 to 300 rpm), and positive (0 to 1300 rpm). These ranges were chosen to reflect the dynamic response characteristics of the motor and to ensure sufficient overlap between sets, which was essential for achieving smooth control transitions.

The triangular membership function is defined mathematically as (3), where a, b, and c represent the lower bound, the peak (or the point of full membership), and the upper bound of the fuzzy set, respectively. Meanwhile, x is the crisp input value, and $\mu_A(x)$ is the degree of membership of x in fuzzy set A, ranging from 0 to 1.

$$\mu_A(x) = \begin{cases} 0 & x \le a \text{ atau } x \ge c \\ \frac{(x-a)}{(b-a)}, & a < x \le b \\ \frac{(c-x)}{(c-b)}, & b < x < c \end{cases} \quad (3)$$

Triangular membership functions were selected primarily due to their computational simplicity, making them highly suitable for real-time implementation using PLC ladder logic. Unlike Gaussian or trapezoidal functions, triangular functions can be efficiently evaluated using basic arithmetic operations such as addition, subtraction, and division—operations that are well supported by the instruction set of the GX Works2 software used in the Mitsubishi FX3U-64M PLC. This choice ensures a balance between performance and accuracy without overloading the limited computational resources of the PLC.

Figure 3 depicts the input membership functions for both $E(k)$ and $\Delta E(k)$. Each input generated three overlapping triangular regions corresponding to negative, zero, and positive linguistic terms. The overlapping structure ensured smooth transitions between adjacent fuzzy states and prevented abrupt control actions, thereby contributing to the robustness of the fuzzy inference process.

On the other hand, the output variable, denoted as digital value (DV), also employed a triangular membership function to map fuzzy inference results into control signals. The DV output was partitioned into three fuzzy sets: negative (−3503 to 0), zero (−800 to 800), and positive (0 to 3503), as depicted in Figure 4. These values were scaled to match the 12-bit digital resolution of the FX2N-2DA DAC module, ensuring precise analog voltage output ranging from 0 to 10 V. This analog voltage directly controlled the input of the FR-E520 inverter, adjusting the frequency and amplitude of the voltage supplied to the motor.

In implementation, each fuzzy input was processed to yield three membership degrees, represented as scaled integer values (0–1000) to accommodate the PLC's integer-based computation. These values were then used within the inference engine to evaluate the fuzzy rules. The accurate construction and mapping of these membership functions, as shown in Figure 3 and Figure 4, are fundamental to the controller's ability to interpret variations in speed error and generate appropriate real-time control signals, ensuring stable and adaptive performance under dynamic load conditions.

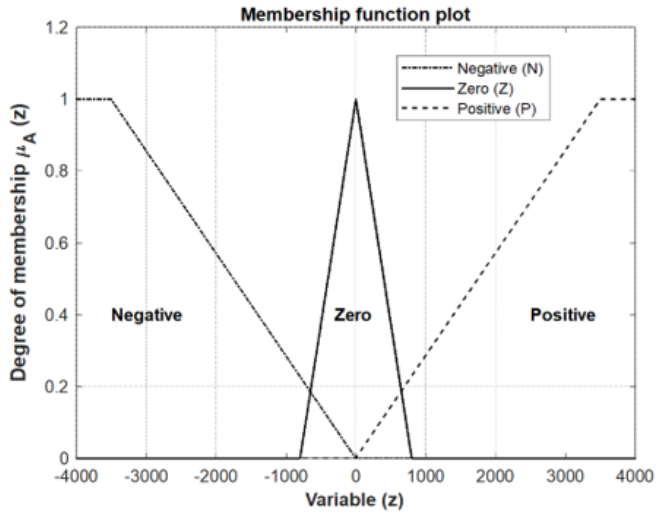

Figure 4. Triangular membership functions for the output variable digital value (DV).

3) INFERENCE PROCESS

The fuzzified input variables, namely the instantaneous speed error $E(k)$ and the change in error $\Delta E(k)$, were processed through a fuzzy inference mechanism employing a structured set of nine IF–THEN rules. These rules were derived from the transient response behavior of three-phase induction motors, which inherently exhibited nonlinearities, time delays, and sensitivity to mechanical load disturbances. The inference structure was designed to translate variations in system dynamics into corrective control actions for motor speed regulation.

Figure 5 depicts the transient speed response of the three-phase induction motor under varying control actions, providing an intuitive understanding of how different combinations of error and delta error affect the system's behavior. This figure serves as the qualitative basis for the formulation of the fuzzy rule set, mapping specific dynamic conditions (e.g., increasing error, decreasing error, overshoot) to appropriate output control actions. By analyzing these transient patterns, the control strategy can be tailored to achieve faster recovery times, minimal overshoot, and reduced steady-state error. The complete set of fuzzy rules is systematically presented in Table I, which functions as the decision matrix of the fuzzy inference engine. The table cross-references the linguistic values of $E(k)$ (rows) and $\Delta E(k)$ (columns), resulting in a 3×3 rule matrix with output recommendations for each possible input pair.

Through the combined functionality of Figure 5 and Table I, the inference engine captured both the qualitative dynamics of motor behavior and the quantitative rule mapping, enabling real-time decision-making under varying load conditions. This approach eliminated the need for precise mathematical modelling and allowed the controller to adaptively handle system uncertainties, ensuring smooth, stable, and efficient speed regulation in industrial environments.

In this study, the Mamdani inference method was utilized to evaluate the fuzzy rule base and generate appropriate control actions. This method applied the minimum (min) operator to represent the logical conjunction (AND) between fuzzy input variables and the maximum (max) operator to aggregate the outputs of multiple rules. Specifically, the activation degree of each fuzzy rule was determined by taking the minimum value between the membership degrees of the two input variables—error and change in error—associated with a given rule.

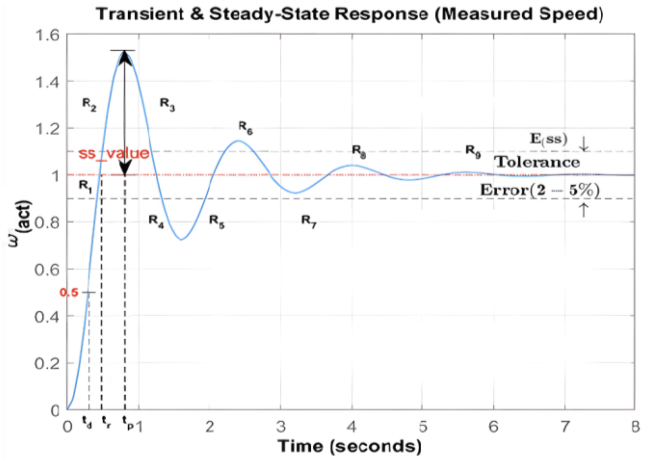

Figure 5. Transient response of the three-phase induction motor speed system.

TABLE I
FUZZY RULE BASE FOR MOTOR SPEED CONTROL

ΔE/E	Negative (N)	Zero (Z)	Positive (Z)
Negative (N)	Negative (N)	Negative (N)	Zero (Z)
Zero (Z)	Negative (N)	Zero (Z)	Positive (P)
Positive (P)	Zero (Z)	Positive (P)	Positive (P)

Mathematically, the activation degree of the *i*th rule is expressed as in (4) [17]–[19].

$$\mu_{\text{active}}^{(i)} = \min\left(\mu_E^{(j)}, \mu_{\Delta E}^{(k)}\right) \tag{4}$$

where $\mu_E^{(j)}$ is the membership degree of the error variable in category j, $\mu_{\Delta E}^{(j)}$ is the membership degree of the delta error in category k, and $\mu_{\text{active}}^{(i)}$ is the resulting activation level of rule i. In situations where multiple fuzzy rules yielded outputs associated with the same output category, their respective activation degrees were combined using the maximum (max) operator. This aggregation process produces a single, unified membership value for each output category, as described by (5):

$$\mu_{\text{output}}(z)=\max(\mu_1(z), \mu_2(z), \ldots, \mu_9(z)). \tag{5}$$

This inference mechanism ensures that the fuzzy controller can effectively interpret complex input scenarios and deliver consistent, reliable control actions based on a well-defined set of fuzzy rules.

Within the PLC implementation, each fuzzy rule was constructed as a block of relational logic using ladder diagram programming. The membership degrees resulting from the fuzzification stage were represented as integer values ranging from 0 to 1000, making them suitable for processing using the PLC's integer arithmetic and comparison instructions. These values were evaluated and aggregated in real time, and the resulting fuzzy outputs were temporarily stored in the controller's memory. This allowed for seamless transition into the defuzzification phase, where a crisp control signal was ultimately derived and used to regulate the system's behavior.

4) DEFUZZIFICATION

Defuzzification is the process of converting the aggregated fuzzy output into a crisp control value, which is essential for interfacing with physical system components. In this study, the centroid method—also known as the center of gravity approach—was employed to perform defuzzification. This

method computes the crisp output u as a weighted average of the output membership functions, using (6) [20].

$$u = \frac{\sum_{i=1}^{n} \mu_i(z_i) \cdot z_i}{\sum_{i=1}^{n} \mu_i(z_i)} \quad (6)$$

where u represents the crisp output value, z_i is the center of the ith output membership function, $\mu_i(z_i)$ is the corresponding membership degree, and n is the number of active fuzzy rules. The result of this calculation was a single numeric value that effectively represented the combined influence of all applicable fuzzy rules. This crisp output was then transmitted to the FX2N-2DA DAC module, generating a corresponding 0–10 V analog signal. This signal was used by the FR-E520 inverter to adjust the frequency of the voltage supplied to the motor, thereby regulating its speed. The centroid-based defuzzification method ensured that the control action was smooth, continuous, and precise, aligning well with the real-time demands of industrial automation systems.

In the PLC-based implementation, the defuzzification process was adapted into discrete arithmetic operations suitable for real-time ladder logic execution. Each fuzzy output DV was associated with a fixed crisp value on a 12-bit scale (0–4000), ensuring compatibility with the analog output range. The resulting voltage was used by the inverter as the reference to modulate the motor's frequency. Given that motor speed n is directly proportional to frequency f, according to $n = \frac{120 \cdot f}{p}$, the fuzzy controller achieves adaptive and continuous speed regulation by manipulating the input frequency in real time [21].

C. IMPLEMENTATION ON PLC

The implementation of the fuzzy logic control system was fully realized within the Mitsubishi FX3U-64M PLC using ladder diagram programming via GX Works2 software. This approach enables adaptive fuzzy control without relying on external software platforms such as MATLAB or LabVIEW, thereby enhancing system efficiency and simplifying integration into existing industrial automation environments.

The control algorithm was structured into modular functional blocks, each responsible for a specific stage of the control process. The first block calculated the actual motor speed based on pulse signals received from a rotary encoder connected to the high-speed counter input of the PLC. This measured speed was then used to compute two critical parameters of the fuzzy control system: the error (E) and the change in error (ΔE). These computations were executed using arithmetic blocks embedded within the ladder logic. To clarify the practical implementation, the calculation of motor speed from the rotary encoder pulses was realized using a high-speed counter input block in GX Works2. The corresponding ladder diagram is shown in Figure 6.

In the subsequent fuzzification stage, the crisp values of error and delta error were mapped into fuzzy sets using triangular membership functions. Each input was categorized into three linguistic variables: negative (N), zero (Z), and positive (P). The inference mechanism evaluated the combination of E and ΔE based on a rule base consisting of nine fuzzy IF-THEN rules, implemented using the min-max inference method.

The result of the inference process was a fuzzy output, which was then processed through defuzzification using the weighted average method. The resulting crisp control signal was scaled and converted into a 12-bit digital value

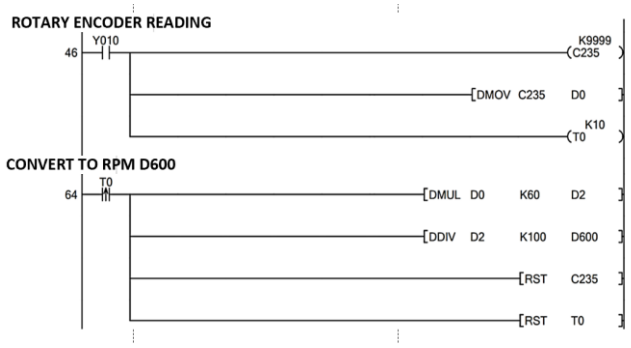

Figure 6. Speed counter programming.

corresponding to the input range of the FX2N-2DA DAC. The DAC subsequently transformed this digital value into an analog voltage in the 0–10 V range, which was then used to modulate the output frequency of the Mitsubishi FR-E520 inverter [22].

All stages of the fuzzy control process, including sensor signal acquisition, fuzzy computation, and control signal generation, were executed internally by the PLC without any external intervention. This fully embedded architecture not only simplified the system design but also enhanced system reliability and responsiveness to dynamic load changes. As a result, the developed control system exhibited adaptive behavior, stability, and reliability, making it suitable for practical industrial applications.

III. TESTING PROCEDURE AND EXPERIMENTAL DESIGN

To evaluate the performance of the fuzzy logic control system implemented on the Mitsubishi FX3U-64M PLC [23], a series of experimental tests were conducted under two primary operating conditions: no-load and loaded scenarios. The objective of these tests was to assess the system's capability to maintain stable speed in a three-phase induction motor under dynamic load variations in real time and to evaluate performance characteristics such as steady-state error and recovery time.

In the first test scenario, the system was operated under no-load conditions, with three different speed set points: 800 rpm, 1000 rpm, and 1200 rpm. This phase aimed to analyze the control system's accuracy and response under standard conditions, free from external mechanical load interference. The actual motor speed was continuously monitored using a rotary encoder and compared with the reference set points to evaluate the precision and stability of the fuzzy logic controller.

The second set of experiments involved applying mechanical loads to the motor shaft by introducing frictional resistance proportional to masses of 0.5 kg, 1.0 kg, and 1.5 kg. During this test, the set point speed was maintained at 1000 rpm. The goal was to examine the controller's adaptive capability in responding to load-induced torque variations and to determine how effectively the fuzzy logic algorithm, embedded within the PLC, can maintain speed stability.

To evaluate the performance of the proposed control system, two key performance indicators were utilized: steady-state error and recovery time. The steady-state error (E_{ss}) is defined as the absolute difference between the actual motor speed and the reference set point once the system has reached a stable operating condition. This metric serves as a critical indicator of the final control accuracy achieved by the system. Meanwhile, the recovery (t_s) refers to the duration required for the system to reach and consistently remain within a ±2% tolerance band around the designated set point following a load

disturbance or operational transition. This measure reflects the dynamic responsiveness of the control system in adapting to changes and restoring desired performance levels efficiently.

Motor speed data, control signals, and process variables were visualized in real time through the GOT1000 HMI, which also served as the interface for configuring set points and monitoring system behavior [24]. The experimental framework was carefully designed to replicate actual industrial conditions, ensuring that the results obtained are representative of the system's real-world performance in practical automation environments.

IV. RESULTS AND EVALUATION

The fuzzy control system was experimentally tested to evaluate its performance in regulating the speed of a three-phase induction motor under varying load conditions, including both no-load and loaded scenarios. The evaluation was centered around two key performance metrics: steady-state error (E_{ss}) and settling time (t_s). For clarity and completeness, the experimental results are presented in both tabular and graphical formats.

A. PERFORMANCE UNDER NO-LOAD CONDITION

The initial experimental validation of the fuzzy logic-based speed control system was performed under no-load operating conditions, in which the three-phase induction motor was run without any mechanical load applied to the shaft. During this phase, five distinct motor speed set points were tested: 300 rpm, 500 rpm, 800 rpm, 1000 rpm, and 1200 rpm. The objective of this test was to evaluate the controller's ability to track varying reference speeds accurately and to assess the system's response time and stability in the absence of external disturbances.

A detailed summary of the experimental outcomes is provided in Table II, which presents four key performance metrics for each test case: the speed set point, the actual steady-state speed achieved, the settling time (t_s), and the steady-state error (E_{ss}) expressed as a percentage. The steady-state error is calculated as the absolute difference between the actual motor speed and the reference set point once the system reaches equilibrium, while the settling time is defined as the duration required for the motor to enter and remain within a ±2% tolerance band of the target speed.

The results in Table II clearly show that the fuzzy logic controller was effective in driving the motor to the desired speed with high accuracy. Across all test points, the steady-state error remained consistently below 1%, indicating that the system achieved precise speed regulation under nominal conditions. Furthermore, the average settling time across all tests was approximately 4.65 s, which is acceptable for real-time industrial applications. The system exhibited no significant overshoot or oscillatory behavior, highlighting the robustness and stability of the control strategy.

To complement the numerical data, Figure 7 depicts a real-time visualization of the system response during the no-load tests, as captured through the GOT1000 HMI. This figure illustrates the dynamic tracking behavior of the motor speed relative to the set point. The smooth and monotonic rise of the speed curve without excessive fluctuations confirms the effectiveness of the fuzzy control algorithm in managing motor acceleration and deceleration in a stable manner. The HMI display not only visualizes the actual versus reference speed but also reflects the system's internal states, offering valuable insights into real-time control behavior.

TABLE II
NO-LOAD TEST RESULTS

Set Point Speed (rpm)	Actual Speed (rpm)	Settling Time, *ts* (s)	Steady-State Error, *Ess* (%)
300	305	2.25	0.67
500	400	3	0.5
800	790	5.25	0.44
1,000	988	6	0.45
1,200	1,185	6.75	0.36

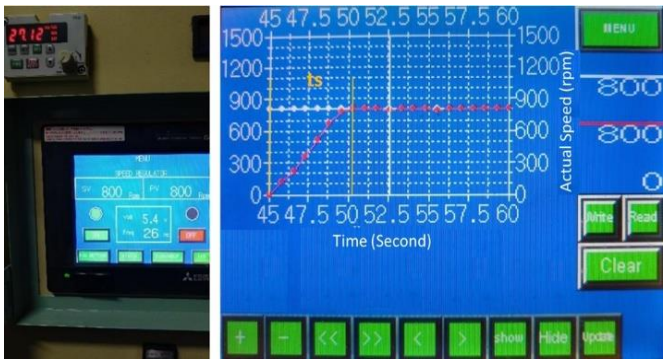

Figure 7. Transient speed response of the induction motor at 800 rpm (no load condition).

B. SYSTEM RESPONSE TO LOAD VARIATIONS

Following the no-load performance evaluation, additional experiments were conducted to assess the dynamic adaptability of the fuzzy logic speed control system under varying mechanical load conditions. In this phase, a constant reference speed of 1000 rpm was maintained, while external frictional loads of 0.5 kg, 1.0 kg, and 1.5 kg were sequentially applied to the motor shaft to simulate realistic operational disturbances. This test aimed to examine the controller's ability to respond to torque fluctuations and maintain speed regulation accuracy in the presence of additional mechanical inertia.

The quantitative results of these tests are presented in Table III, which summarizes four key performance indicators for each applied load: the constant speed set point (1000 rpm), the actual steady-state speed achieved after load application, the settling time (t_s) required to restabilize the speed within the ±2% tolerance band, and the steady-state error (E_{ss}) expressed as a percentage. These metrics provide critical insight into the control system's robustness, compensatory capability, and transient recovery performance under load-induced disturbances.

Analysis of Table III shows that the fuzzy logic controller maintained high regulation accuracy across all load conditions, with steady-state errors remaining below 0.5%. Notably, the system demonstrated fast recovery characteristics, with settling times averaging only 1.5 s, which is significantly shorter than the no-load condition. This behavior highlights the effectiveness of the fuzzy control logic in adapting to sudden torque variations and re-establishing the desired operating point rapidly.

To complement the numerical evaluation, Figure 8 shows a real-time graphical visualization of the system response under a 1.0 kg load at 800 rpm. The figure displays the time-domain speed trajectory as monitored via the GOT1000 HMI. The plotted data showed a brief transient deviation immediately after load application, followed by a smooth, rapid convergence to the set point. There was no evidence of excessive overshoot or sustained oscillation, indicating that the fuzzy logic

TABLE III
LOAD TEST RESULTS

Load (kg)	Set Point Speed (rpm)	Actual Speed (rpm)	Settling Time, *ts* (s)	Steady-State Error, *Ess* (%)
0.5	1,000	998	1.5	0.3
1.0	1,000	994	1.5	0.4
1.5	1,000	998	1.5	0.35

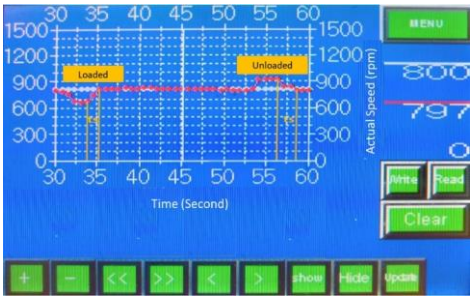

Figure 8. Transient speed response at 800 rpm under 1 kg load condition.

controller effectively absorbs disturbances and re-stabilizes the system in real time.

C. INDUSTRIAL IMPLEMENTATION ASSESSMENT

In addition to its dynamic performance, the fuzzy logic speed control system demonstrated strong potential for industrial implementation. The entire control algorithm was embedded directly within the Mitsubishi FX3U-64M PLC, removing the need for external software platforms such as MATLAB or additional controllers. This simplified the system architecture, reduced cost and complexity, and improved long-term reliability in industrial environments.

The use of the GOT1000 HMI further enhanced the practicality of the system. Operators were able to set speed targets, monitor real-time motor response, and observe control performance without external devices. As shown in Figure 7 and Figure 8, the HMI provides clear visualization of motor speed behavior, making the system easy to supervise and maintain.

Testing under no-load conditions (Table II) showed that the system consistently reached the desired speed set points with steady-state errors below 1% and average settling times around 4.65 s. These results confirm accurate and stable control under nominal conditions.

More importantly, under loaded conditions (Table III), where external loads of 0.5 to 1.5 kg were applied, the controller still maintained high precision, with steady-state errors below 0.5% and faster settling times, averaging just 1.5 s. This demonstrates the system's ability to respond quickly and effectively to sudden changes in torque, a key requirement in many industrial applications.

Overall, the consistent performance across both test scenarios confirms that the fuzzy logic controller is not only effective but also ready for real industrial deployment. Its compact implementation, fast response, and ease of integration make it well-suited for environments that demand reliable and adaptive speed control, especially in systems subject to varying mechanical loads.

V. CONCLUSION

This research demonstrates the successful implementation of a fully embedded fuzzy logic-based speed control system for a three-phase induction motor using the Mitsubishi FX3U-64M PLC. The control algorithm, comprising fuzzification, inference, and defuzzification stages, was developed entirely using ladder logic within the GX Works2 platform, without the need for external computational tools. Experimental evaluations under both no-load and variable mechanical load conditions revealed that the system was capable of maintaining high speed regulation accuracy, with steady-state errors remaining below 1% in no-load scenarios and below 0.5% under load conditions. Furthermore, the system exhibited fast transient response, with settling times between 1.5 and 6.75 s depending on the operating condition. The integration of real-time monitoring via the GOT1000 HMI further enhances the system's practical applicability in industrial environments. These findings substantiate that the proposed fuzzy control scheme provides a compact, adaptive, and reliable solution for real-time motor speed regulation. Its consistent performance under both steady and dynamic loading conditions highlights its strong potential for integration into industrial automation systems characterized by varying operational demands and load sensitivities.

CONFLICTS OF INTEREST

The authors declare that there is no conflict of interest with any party regarding the conduct of this research, data analysis, or the preparation of this manuscript.

AUTHORS' CONTRIBUTIONS

Conceptualization, Nanang Rohadi and Liu Kin Men; methodology, Nanang Rohadi; software, Nanang Rohadi; validation, Nanang Rohadi, Liu Kin Men, and Akik Hidayat; formal analysis, Nanang Rohadi; investigation, Nanang Rohadi; resources, Nanang Rohadi; data curation, Nanang Rohadi ; writing—original draft preparation, Nanang Rohadi; writing—reviewing and editing, Nanang Rohadi; visualization, Nanang Rohadi; supervision, Nanang Rohadi; project administration, Nanang Rohadi; funding acquisition, Liu Kin Men.

ACKNOWLEDGMENT

The authors would like to express their gratitude to the Electrical Engineering Laboratory, Faculty of Mathematics and Natural Sciences, Universitas Padjadjaran, for providing technical and facility support throughout the research. Appreciation is also extended to colleagues who offered constructive feedback during the system development and manuscript preparation.

REFERENCES

[1] V.D. Nguyen *et al.,* "A Combination of Fourier transform and machine learning for fault detection and diagnosis of induction motors," in *2021 8th Int. Conf. Dependable Syst. Their Appl. (DSA)*, 2021, pp. 344–351, doi: 10.1109/DSA52907.2021.00053.

[2] H. Nory, A. Yildiz, S. Aksun, and C. Aksoy, "Influence of stator and rotor slots combination on induction motor performance," in *2024 IEEE 3rd Int. Conf. Power Electron. Intell. Control Energy Syst. (ICPEICES),* 2024, pp. 177–181, doi: 10.1109/ICPEICES62430.2024.10719270.

[3] Z. Anthony *et al.,* "Improving the performance of 3-phase induction motors by developing a symmetrical 6-phase winding design on the motor," in *2023 Int. Conf. Eng. Technol. Technopreneursh. (ICE2T)*, 2023, pp. 1–5, doi: 10.1109/ICE2T58637.2023.10540496.

[4] J. Bonet-Jara, V. Fernandez-Cavero, F. Vedreno-Santos, and J. Pons-Llinares, "Very accurate time-frequency representation of induction motors harmonics for fault diagnosis under arbitrary load variations," in *2022 Int. Conf. Elect. Mach. (ICEM),* 2022, pp. 1517–1523, doi: 10.1109/ICEM51905.2022.9910768.

[5] R.S.Y and M.N. Sujatha, "Performance evaluation of traction motor through load and no-load testing for industrial applications," in *2024*

Glob. Conf. Commun. Inf. Technol. (GCCIT), 2024, pp. 1–4, doi: 10.1109/GCCIT63234.2024.10862152.

[6] O. Faiz and B. Noureddine, "Discrimination between broken bars fault and load torque variation in induction motors," in *2022 Int. Conf. Commun. Inf. Electron. Energy Syst. (CIEES)*, 2022, pp. 1–6, doi: 10.1109/CIEES55704.2022.9990889.

[7] J.M. Tabora *et al.,* "Efficient electric motors performance under voltage variation conditions," in *2023 IEEE Kans. Power Energy Conf. (KPEC),* 2023, pp. 1–6, doi: 10.1109/KPEC58008.2023.10215475.

[8] Y. Zhang, Z. Zhao, and H. Zhang, "Performance assessment and self-healing of PID controller based on model adaption with ZNN," in *2021 33rd Chin. Control Decis. Conf. (CCDC)*, 2021, pp. 5000–5005, doi: 10.1109/CCDC52312.2021.9602296.

[9] W. Wei, G. Jiajun, and F. Peng, "Modeling method of marine diesel generator based on Fuzzy PID control," in *2020 7th Int. Conf. Inf. Sci. Control Eng. (ICISCE),* 2020, pp. 1939–1943, doi: 10.1109/ICISCE50968.2020.00381.

[10] Y. Ren, Z. Zhao, C.K. Ahn, and H.-X. Li, "Adaptive fuzzy control for an uncertain axially moving slung-load cable system of a hovering helicopter with actuator fault," *IEEE Trans. Fuzzy Syst.,* vol. 30, no. 11, pp. 4915–4925, Nov. 2022, doi: 10.1109/TFUZZ.2022.3164512.

[11] B. Gao *et al.,* "The simulation of direct torque control fuzzy control system based on Labview and Matlab," in *2014 2nd Int. Conf. Syst. Inform. (ICSAI 2014),* 2014, pp. 94–98, doi: 10.1109/ICSAI.2014.7009266.

[12] G. Cui and R. Li, "Stability analysis and optimization strategy of PLC ship lock system based on fuzzy logic control," in *2025 Int. Conf. Elect. Drives Power Electron. Eng. (EDPEE)*, 2025, pp. 1439–1443, doi: 10.1109/EDPEE65754.2025.00259.

[13] S. Yordanova, M. Slavov, G. Prokopiev, and D. Stoitseva-Delicheva, "Industrial bound design and application of fuzzy logic PID controller for liquid level in carbonisation column," in *2022 Int. Conf. Autom. Inform. (ICAI),* 2022, pp. 210–217, doi: 10.1109/ICAI55857.2022.9960121.

[14] R. Yu, Y.-H. Chen, B. Han, and H. Zhao, "A hierarchical control design framework for fuzzy mechanical systems with high-order uncertainty bound," *IEEE Trans. Fuzzy Syst.*, vol. 29, no. 4, pp. 820–832, Apr. 2021, doi: 10.1109/TFUZZ.2020.2965913.

[15] R. Yu *et al.,* "Robust control design for fuzzy mechanical systems: A two-player Nash game approach," *IEEE Trans. Syst. Man Cybern., Syst.*, vol. 52, no. 10, pp. 6569–6581, Oct. 2022, doi: 10.1109/TSMC.2022.3147255.

[16] R. Musil, R. Farana, R. Rouš, and Š. Bilík, "Fuzzy controller tuning methods for typical plant types," in *2024 21st Int. Conf. Mechatron. - Mechatronika (ME),* 2024, pp. 1–4, doi: 10.1109/ME61309.2024.10789767.

[17] L.T.H Lan *et al.,* "A new complex fuzzy inference system with fuzzy knowledge graph and extensions in decision making," *IEEE Access,* vol. 8, pp. 164899–164921, Sep. 2020, doi: 10.1109/ACCESS.2020.3021097.

[18] X. Zhao and F. Guo, "Normalization: A tool for controlling concentration effects in fuzzy set aggregation," in *2024 6th Int. Conf. Elect. Eng. Control Technol. (CEECT),* 2024, pp. 67–75, doi: 10.1109/CEECT63656.2024.10898344.

[19] G. Xue, J. Wang, K. Zhang, and N.R. Pal, "High-dimensional fuzzy inference systems," *IEEE Trans. Syst. Man Cybern.,* vol. 54, no. 1, pp. 507–519, Jan. 2024, doi: 10.1109/TSMC.2023.3311475.

[20] A.K. Mallick and A. Das, "An Analytical survey of defuzzification techniques," in *2021 IEEE 4th Int. Conf. Comput. Power Commun. Technol. (GUCON)*, 2021, pp. 1–6, doi: 10.1109/GUCON50781.2021.9573993.

[21] S.V. Joshi, P.S., and M.S., "Fuzzy logic based speed control of induction motor using SVPWM technique," in *2025 Int. Conf. Intell. Innov. Technol. Comput. Elect. Electron. (IITCEE),* 2025, pp. 1–6, doi: 10.1109/IITCEE64140.2025.10915418.

[22] *FR-E520 Inverter Product Specifications*, Mitsubishi Electric Co., Tokyo, Japan, 1999.

[23] *Base Units FX3U Series*, Mitsubishi Electric Co., Tokyo, Japan, 2009.

[24] *Mitsubishi Graphic Operation Terminal GOT1000 Series*, Mitsubishi Electric Co., Tokyo, Japan, 2012.